

Chapter 5

Phase separation of passive colloidal particles in active suspensions of bacteria

5.1 Introduction

In the previous Chapter 4, we have studied the effect of chirality. We observe on the basis of chirality we have different phases in the system. On varying chirality we have macrophase, then for intermediate value of chirality microphase, further increasing the value of chirality homogeneous phase observed in the system. Here, we present the results of a research of passive colloids distributed in bacterial active suspensions using experimental and computational methods. The computational part of this problem is part of this thesis done by me.

For more than a century, the Brownian motion of colloidal particles has captured our attention [Bechinger et al. \(2016\)](#); [Romanczuk et al. \(2012\)](#). The particles exhibit an endless random motion when dispersed in liquids because of frequent collisions with the solvent molecules. Ensembles of colloidal particles are known to self-assemble and display a broad range of phases based on their shapes and interactions as a result of temperature fluctuations and interactions. It is well known that the equilibrium statistical mechanics

principles govern the phase behaviour of these systems. In contrast, the phase behavior of colloidal particles in nonequilibrium systems has received little attention [Bechinger et al. (2016); Romanczuk et al. (2012); Shaebani et al. (2020)]. Active matter systems represent a large class of nonequilibrium systems that are comprised of self-propelled units, such as bacteria, animals, birds, molecular motors, synthetic colloids and others, which consume energy and perform directed motion [Ramaswamy et al. (2003)]. They are known to exhibit a variety of fascinating occurrences, including flocking [Cavagna & Giardina (2014)], and motility induced phase separation [Bechinger et al. (2016); Cates & Tailleur (2015); Kümmel et al. (2013); Marchetti et al. (2013); Shaebani et al. (2020)], active turbulence etc. Therefore, active matter systems provide new methods for systems that are out of equilibrium. We looked into the phase behaviour of colloidal particles dispersed in active liquid [Patteson et al. (2016)].

5.2 Model

The simulations were performed with a binary mixture that contained N_a small active particles of radius a_a and N_p big passive particles of radius a_p ($a_p > a_a$) moving on a two dimensional frictional substrate. The active particles are associated with a self propulsion speed v and an orientation vector that is represented by a unit vector $\hat{v}_i = (\cos\theta_i; \sin\theta_i)$, where θ_i is the angle between the velocity vector and a reference direction. The motion of active Brownian particles (ABP) is governed by the following Langevin equations [Marchetti et al. (2013); Semwal et al. (2021)]:

$$\frac{d\mathbf{r}_i}{dt} = v\hat{v}_i - \mu_1 \sum_{j \neq i} \mathbf{F}_{ij} + \sqrt{2D_T} \eta_{Ti} \quad (5.1)$$

$$\frac{d\theta_i}{dt} = \Gamma \sum_j \sin(\theta_i - \theta_{ij}) + \sqrt{2D_r} \eta_{ri}. \quad (5.2)$$

Here μ_1 is the mobility and \mathbf{F}_{ij} is the force acting on particle i due to particle j . The noise term is defined as $\langle \eta_{r,Ti}(t)\eta_{r,Tj}(t') \rangle = 2D_{r,T}\delta_{ij}\delta(t-t')$, D_T and D_r are the translational and rotational diffusion constants of active particles and Γ is the magnitude of alignment and $\theta_{ij} = \arg(\mathbf{r}_i - \mathbf{r}_j)$. The inverse of the rotational diffusion D_r^{-1} is the time scale over which the orientation of an active particle changes. Hence, $l_p = v/D_r$ is the persistence length or run length, which is the typical distance travelled by an active particle before it changes direction. It is constant in our study, and is set to $l_p = 20a_a$, $D_T = 0.005$.

The equation of motion for passive particles is

$$\frac{d\mathbf{r}_i}{dt} = \mu_2 \sum_{j \neq i} \mathbf{F}_{ij}, \quad (5.3)$$

where μ_2 is the mobility of passive particles. There is no translational noise in eqn. 5.3 hence the dynamics of passive particles is only due to interaction force. We choose the mobility of both species to be the same i.e., $\mu_1 = \mu_2$. Particles interact through short ranged soft repulsive forces $\mathbf{F}_{ij} = F_{ij}\hat{\mathbf{r}}_{ij}$, where $F_{ij} = k(a_i + a_j - r_{ij})$ when $r_{ij} \leq (a_i + a_j)$ and $F_{ij} = 0$ otherwise; $r_{ij} = |\mathbf{r}_i - \mathbf{r}_j|$ and k is a constant. The elastic time scale in our system is defined by $(\mu k)^{-1} = (150)^{-1}$.

We simulate the system in a square box of size $l_{box} \times l_{box}$ with periodic boundary conditions varying the area fractions $\phi_a = N_a \pi a_a^2 / l_{box}^2$ and $\phi_p = N_p \pi a_p^2 / l_{box}^2$ of active and passive particles respectively. We start with a random homogeneous distribution of active and passive particles in the box and with random directions for the velocity of active particles. Eqn. (5.1-5.3) are updated for all particles and one simulation step is counted after a single update for all the particles. The system is defined by the packing fractions ϕ_a and ϕ_p of the active and passive particles respectively, the activity v of active particles and the size ratio ($S = a_p/a_a$) defined as the ratio of the radius of a passive particle to the radius of an active particle. The system is studied for $\Gamma = 1.0$. We scale the activity by $a_a D_r$ to make it dimensionless and define the Peclet number $Pe = \frac{v}{2a_a D_r}$. It is to be

noted that our simulations does not include the hydrodynamic interactions that are present in experiments. Nevertheless, it sheds new lights on some of the important competing interactions in the system. The effect of hydrodynamic interaction can be included using coarse-grained studies similar to [Cates (2012); Cates & Tailleur (2013, 2015)].

5.3 Effective Potential between Passive Particles

The first quantity that we have calculated in the simulations is the effective potential between two passive particles in the medium of ABPs with torque. In order to calculate the effective potential between two passive particles we choose $N_p = 2$ at positions \vec{r}_1 and \vec{r}_2 , respectively, in a systems of ABPs with $N_a = 1800$. We keep \vec{r}_1 fixed and slowly vary \vec{r}_2 in small steps of $\Delta x = 0.5a_a$ starting from the zero surface to surface distance between two passive particles. The cartoon of the system simulated for the force calculation for a fixed r is shown in Fig. 5.1 (inset). In the figure ABPs are shown in red and passive particles in blue for $S = 8$. For resolution only a part of the system near the two passive particles are shown. The active particles position and orientation is updated according to the eqn. 5.1 and 5.2. For each configuration at a given distance between two passive particles the system is allowed to reach the steady state. Further we use the steady state configuration to calculate the force $\mathcal{F}^S(r)$ between two-passive particles at a surface to surface separation r , such that $\mathcal{F}^S(r) = \mathbf{F}_{12}(r) + \sum_{i=1}^{N_a} \mathbf{F}_{1i}(r)$. Here $\mathbf{F}_{12}(r)$ is the force due to passive particle 2^{nd} on 1^{st} , and $\sum_{i=1}^{N_a} \mathbf{F}_{1i}(r)$ represents the sum of all the forces due to active particles on 1^{st} passive particle for a given configuration of two passive particles at separation r . The potential is then calculated by integrating the force over the distance $U(r) = \int_{-\infty}^r \mathcal{F}^S(r) dr$ [Chakrabarti et al. (2006); Dzubiella et al. (2009); Singh et al. (2022)]. Here we set the lower limit as one fourth of the box-length. To improve the quality of data, 30 independent realisations of the system were considered.

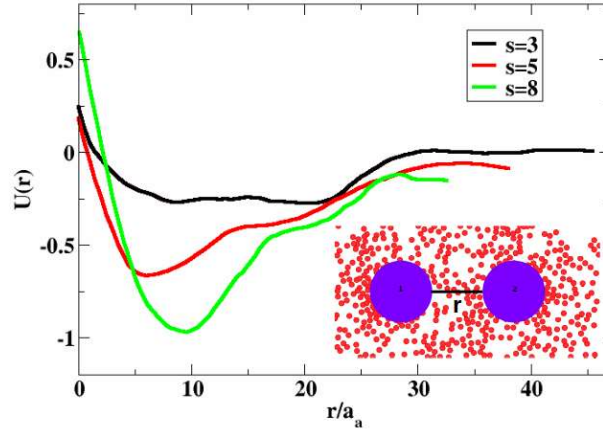


Fig. 5.1 Plot of effective potential $U(r)$ vs. scaled distance for the system for $Pe = 25$ and different size ratios $S = 3, 5$ and 8 . (inset) show the snapshot of a part of the system. The two bigger particles are passive particles. The left particles is marked as particle 1 with position \vec{r}_1 and right is particle 2 with position \vec{r}_2 . The red circles are ABPs. The line shows the surface to surface distance r between two passive particles.

We calculated the effective potentials $U(r)$ for $Pe = 25$ (which is comparable to the experimental system) and three size ratios $S = 3, 5$ and 8 . The comparable size ratio in experimental system is $S \sim (2.5 \text{ to } 5.5)$. We first plot the effective potential $U(r)$. In the Fig. 5.1 we show the plot of $U(r)$ vs. r for the system for size ratios $S = 3, 5$ and 8 . The distance is normalised by the radius of active particles, which is kept fixed to 0.1 . The negative side of the potential shows the attraction and positive nature is repulsion. For all the parameters the potential approaches to zero at large distance, and it is negative at intermediate distances. The depth of the potential becomes deeper with increasing S . To further investigate the effect of such effective potential, full microscopic simulations of mixtures of active and passive were performed using the eqn. 5.1, 5.2, 5.3. We simulated the system for $Pe = 25$ and size ratio $S = 3, 5$ and 8 . In Fig. 5.2(a-c) the steady state snapshots of passive (blue, bigger) and active (red, smaller) are shown for different size ratios $S = 3, 5$ and 8 respectively. Clusters with moderate to strong ordering is found on increasing S . For small $S = 3$ clusters are present but without strong local hexagonal ordering, whereas as we increase S the ordering and clustering is enhanced.

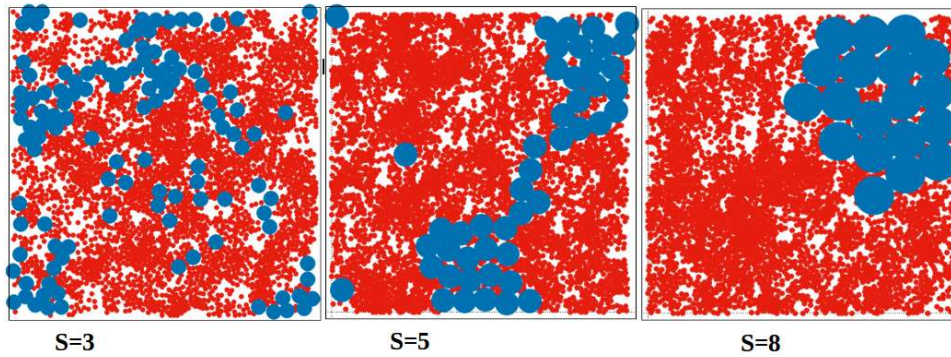


Fig. 5.2 Snapshots of the system obtained from the microscopic simulation: two types of particles for different size ratio $S = 3, 5$ and 8 (left, central and right columns), and $Pe = 25$. Red particles are ABPs and blue particles are passive particles, for fixed packing fraction $\phi = 0.60$ in a system of size $l_{box} = 140a_d$

5.4 Conclusion

The interesting observations that emerge from our studies are that the phase behavior of a seemingly complex system of bacteria, which is strongly out of equilibrium, shows many features that are similar to an equilibrium system with depletion interaction, such as a colloid-polymer mixture [Asakura & Oosawa (1954); Lekkerkerker et al. (1992)]. Even though the emergent interaction in our system is attractive, it appears to be long-ranged, extending to several active particle diameters. So, the origin of this emergent interaction is not clear at present and needs further investigation. The active-passive mixture of bacteria and colloids appears to be a model system to investigate several interesting questions relating to phase separation in living systems where the active processes are known play a dominant role [Berry et al. (2018)]. We believe our results would motivate further study in this direction.
